Compressive strength assessment in additively manufactured sustainable poly lactic acid specimens as per ASTM D695 standard

Yeole Shivraj Narayan[1*], *Kode* Jaya Prakash[1], *Pothula* Narendra[1], *S.* Anand Kumar[1], *Kapish* Barik[1]

[1]Department of Mechanical Engineering, Vallurupalli Nageswara Rao Vignana Jyothi Institute of Engineering and Technology, Hyderabad, India.

Abstract. Relative benefits over traditional manufacturing processes have made fused deposition modeling (FDM)-based 3D printing as prevalent among various fields and sectors. However, the mechanical traits of 3D-printed FDM parts are still a matter of research that primarily depends upon the material used. In addition to acrylonitrile butadiene styrene (ABS) material, another sustainable polymer used in the FDM is polylactic acid (PLA). This study evaluated the compressive strength of 3D-printed PLA specimens consistent with ASTM D695 standard. The test specimens were simulated in ANSYS software to assess the compression strength and deformation of the specimens. Five ASTM specimens were additively manufactured on a Makerbot printer with a 0.3 mm layer resolution, 100% infill rate, 215°C extrusion temperature and standard build speed. The specimens were conditioned in line with ASTM D695 standard. The compressive strengths of the specimens measured on a universal testing machine were correlated with the simulated results. The compressive strength of the specimens was found to be close to the standard strength.

Keywords. Compression testing, Polylactic acid, ASTM D695, 3D printing.

1 Introduction

The 3D printing method is the most advanced method for the manufacturing processes that can deliver and replicate unsupported typical structures in single or multiple components. FDM is a form of additive manufacturing (AM) [1], [2]. Converse to traditional subtractive manufacturing methods, AM can generate complex shapes with reduced assembly costs [3]. The utility of additive manufacturing in the current decade has seen a major hike [4], [5]. Additive manufacturing technology produces parts in the form of layered microstructures independent of shape size and complexity. The mechanical characteristics of AM components rely on the build orientation [6], [7]. The STL file of a CAD model is imported into AM software for the development of the part in layered form to accomplish the final form. The innovation of 3D printing emerges from the normal inkjet desktop printers,

* Corresponding Author: shivrajyeole@vnrvjiet.in

wherein various jets deposit the ink layer after layer in view of the 3D CAD information. This enables designers and creators to go from a level screen to a genuine product [8]. With different parameters impacting the properties of the material and the product quality, FDM is an unpredictable procedure, and it is difficult to understand the combination of these parameters [9], [10]. Variables such as the infill pattern, infill density, layer thickness, raster width, raster angle, feed rate, and part orientation have a considerable influence on the functioning and superiority of AM parts [10], [11], [12], [13], [14], [15], [16]. FDM is based on the notion of manufacturing a product straight from CAD data of the model using a material extrusion process [17].

2 Materials and Methods

2.1 Polylactic Acid

Owing to its affordability, and ease of processing, PLA has become an option for use as a synthetic material in the food industry. It is expected that the production of petrochemical polymers will lessen the impact on the environment [18]. Lower ductility and higher strength of PLA than ABS (Acrylonitrile Butadiene Styrene), biodegradability and eco-friendliness, has made PLA a suitable material for the development of sustainable thermoplastics that reduce waste. PLA has been used extensively in many applications, such as in implants and tissues, due to its biocompatibility [19]. PLA is more brittle than ABS and has a reduced coefficient of thermal expansion, thereby preventing warping of the parts, sticking to the print bed, and cracking of the large parts [20]. Table 1 displays the properties of PLA.

2.2 Design and Modeling of ASTM D695 Specimens

A compression test is a strategy for establishing the behavior of materials under a compressive load. Pressure tests are performed by placing the sample between two plates, followed by the application of force to the sample with the crossheads moving together. This leads to compaction of the sample, allowing recording of distortion values against the connected load. A pressure test is utilized to find the elastic limit, yield point, proportional limit, yield quality, and compressive strength.

Table 1. Properties of PLA ([21], [22], [23], [24], [25], [26])

Property	**Value**
Density (g/cm^3)	1.24
Elongation at break (%)	7.0
Melting temperature, T_m ($^\circ$C)	130-230
Shear modulus, G (MPa)	1287
Elastic modulus, E (MPa)	3500
Rockwell hardness (HRA)	88
Yield strength, σ_y (MPa)	70
Flexural strength, σ_x (MPa)	106
Poisson's ratio, v	0.360
Ultimate tensile strength, σ_{usd} (MPa)	73
Tensile modulus (GPa)	2.7-16
Crystallinity (%)	37
Unnotched izod impact (J/m)	195

A dog-bone specimen with a width of 1.9 cm width and height of 7.94 cm height was designed to meet the h/d ratio criterion of more than 2 needed for compressive testing. CAD

model of the specimen were prepared in conformance to the ASTM D695 standard in SolidWorks software. The dimensions of the specimen and the CAD model are exhibited in Fig. 1 and Fig. 2 respectively.

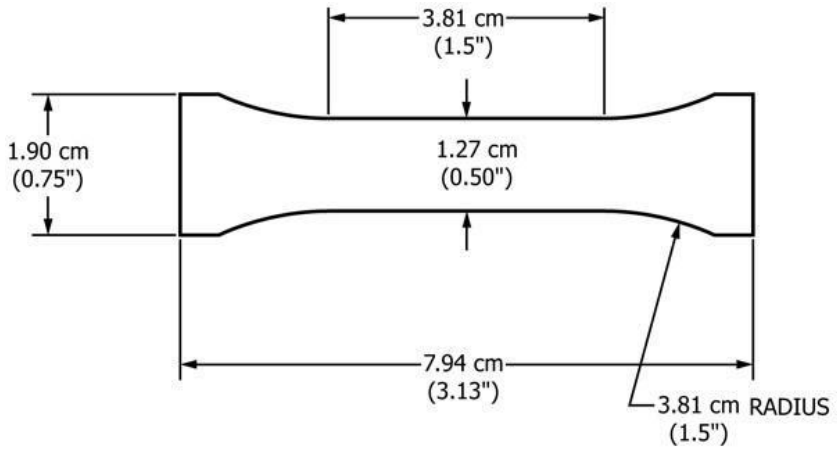

Fig. 1. ASTM D695 compression specimen [27]

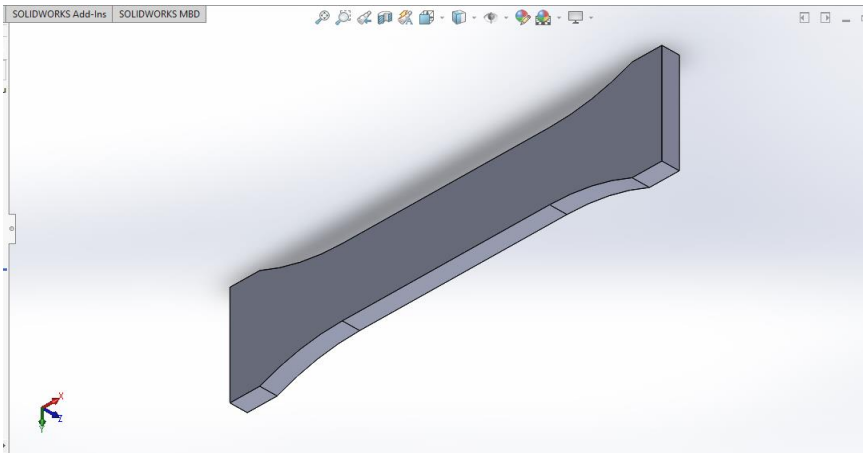

Fig. 2. Designed compression specimen

Fig. 3 displays the STL file model of the compressive specimen. This file is then imported to Autodesk Netfabb software to obtain an error-free file after rectification, as shown in Fig. 4.

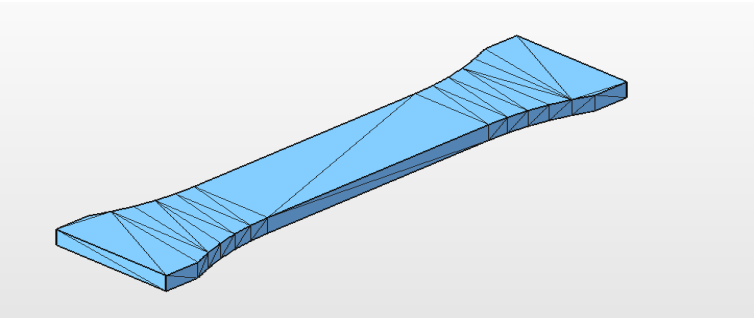

Fig. 3. stl file of compression specimen

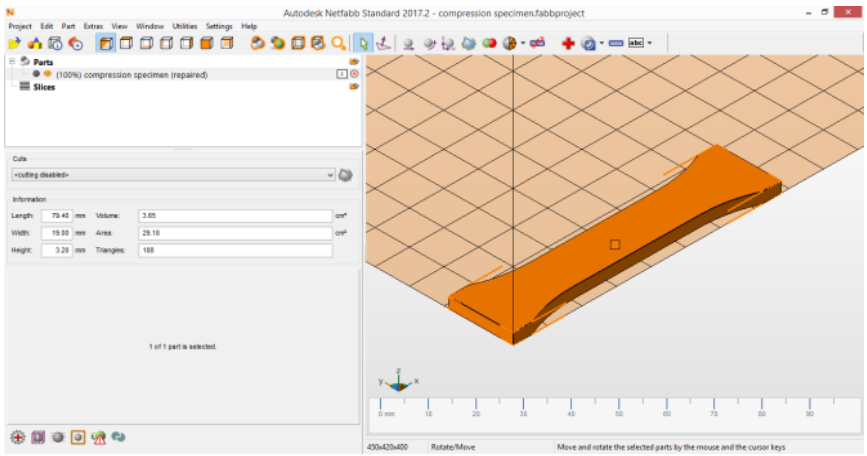

Fig. 4. Imported .stl file of compression specimen in Autodesk Netfabb

2.3 Analysis of Specimens

The compressive strength of the ASTM D695 specimens was virtually simulated using ANSYS structural mechanics workbench software R16.2. Different loads were applied on the specimens for performing stress analysis. Stress was generated in the specimens upon applying compressive loads. Table 2 portrays the stresses generated during the test. A minimum equivalent stress of $1.6175e^6$ N was detected at a load of 196.56 N and a maximum equivalent stress of $1.9144e^7$ N was detected at a load of 713.750 N.

Table 2. Stress induced in compression specimens

Load (N)	Minimum equivalent stress (N/mm^2)	Maximum equivalent stress (N/mm^2)
196.563	$1.6175e^6$	$5.2722e^6$
366.375	$3.0148e^6$	$9.8269e^6$
713.750	$5.8732e^6$	$1.9144e^7$
400.422	$3.2949e^6$	$1.074e^7$
538.125	$4.4281e^6$	$1.4434e^7$

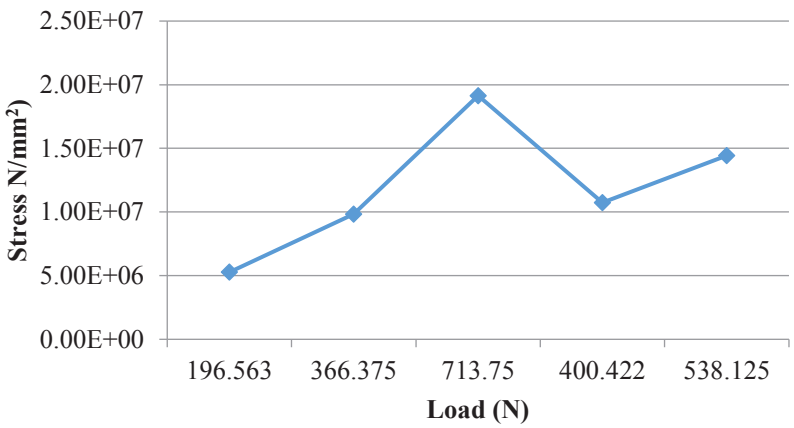

Fig. 5. Stress vs load-compression specimens

Fig. 5 shows the trend of compressive stress in the specimens at various loads. Fig. 6 shows that the gauge length generated greater stress than did the other sections of the specimen. This was attributed to plastic flow or molecular slippage of planes during loading beyond the elastic limit.

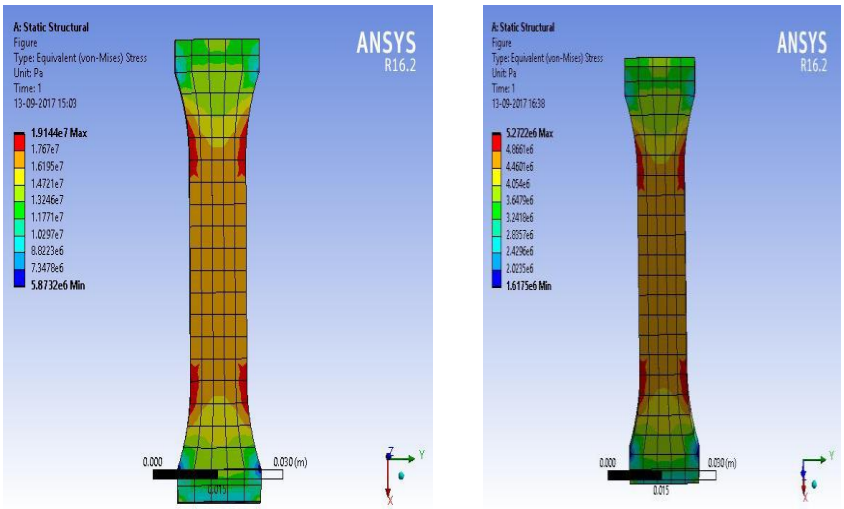

Fig. 6. Maximum and minimum stresses generated in the compression specimens

Similarly, deformation analysis was performed on the specimens at different compressive loads. Table 3 shows the deformation observed at different loads on the specimen. A maximum deformation of 716.78 was noted at a load of 713.75 N.

Table 3. Deformation induced in compression specimens

Load (N)	Minimum deformation (mm)	Maximum deformation (mm)
196.563	0	197.4
366.375	0	367.93
713.750	0	716.78
400.422	0	402.12
538.125	0	540.41

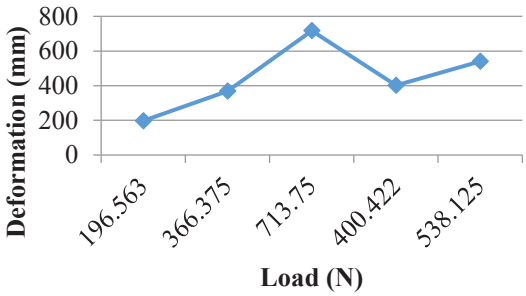

Fig. 7. Deformation vs load-compression specimens

Fig. 7 shows the deformation of the specimens upon application of the load. As shown in Fig. 8, large deformations were detected in the specimen due to the applied load and the external forces acting on it.

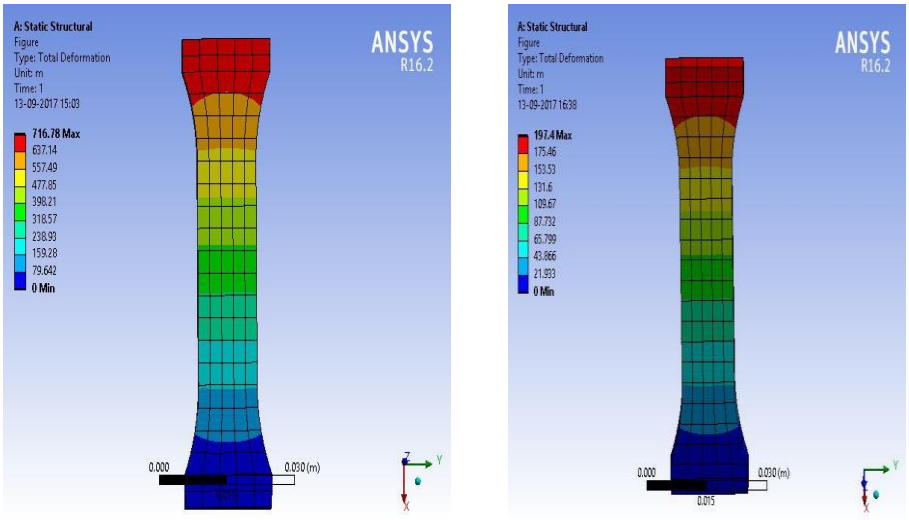

Fig. 8. Maximum and minimum deformation in the compression specimens

Strain analysis was performed on the specimens subjected to various compressive loads. Table 4 shows the maximum and minimum elastic strains achieved during the load testing. At a load of 196.563 N, the minimum elastic strain was noted, whereas the maximum elastic strain was detected at a load of 713.750 N.

Table 4. Strain analysis results of the compression specimens

Load (N)	Minimum elastic strain	Maximum elastic strain
196.563	907.37	2940.8
366.375	1691.2	5481.4
713.750	3294.8	10679
400.422	1848.4	5990.8
538.125	2484.1	8051

Fig. 9 shows the strain instigated in specimens upon applying the load.

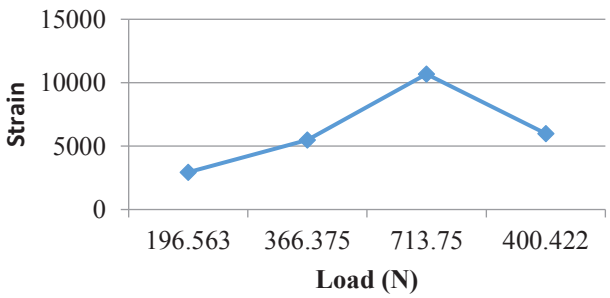

Fig. 9. Strain vs load-compression specimens

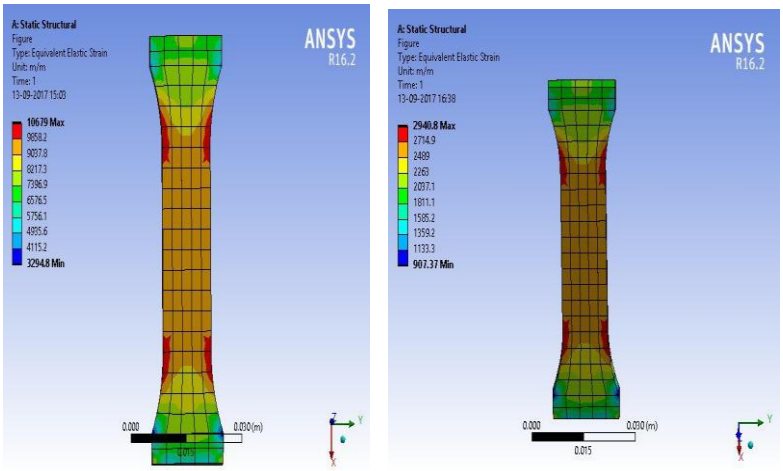

Fig. 10. Maximum and minimum strains in the compression specimens

As depicted in Fig. 10, the strain was greater for the specimen with a gauge length of 713.750 N than for the remaining specimens. Additionally, a decreased specimen length and increased cross-sectional area of the specimen were detected.

2.4 3D Printing of Specimens

Five ASTM D695 complied specimens were additively manufactured using PLA material on Makerbot Replicator Z18 printer. Fig. 11 shows the imported STL file of the model into the Makerware software. The print settings utilized in 3D printing of ASTM specimens is shown in Table 5.

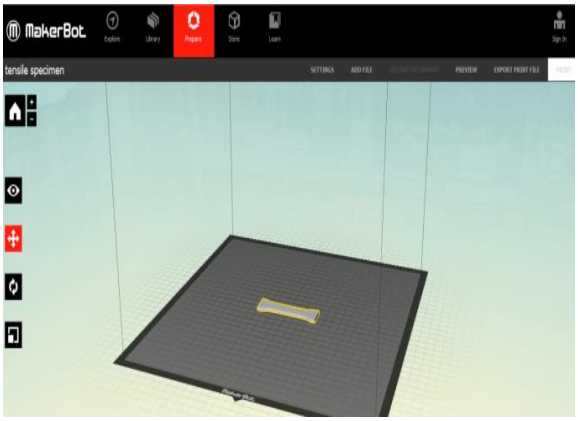

Fig. 11. Imported STL file in the Makerware software

Table. 5 Settings used in 3D printing

Parameter	Value
Layer height (mm)	0.3
Feed rate (mm/sec)	150
Extruder temperature (˚C)	230
Bed temperature (˚C)	110
Number of shells	2
Infill density (%)	100

Fig. 12 shows the 3D-printed ASTM D695 compressive test specimen.

Fig. 12. 3D printed compression specimen

2.5 Experimental Testing on 3D Printed ASTM D695 Specimens

Experimental testing was carried out on an Auto Graph AG 15 Universal Testing Machine (UTM) to analyze the compressive strength of the PLA specimens printed using FDM. A technical description of the UTM machine is presented in Table 6. Test specimens printed in agreement to the ASTM D695 standard were subjected to a 5.0 kN load at a constant crosshead speed of 5 mm/min and a grip distance of 33 mm. The specimens were positioned in the UTM using grippers, a steady load was applied to the specimens until failure, and the consequent loads were recorded.

Table 6. Specifications of UTM

UNIVERSAL TESTING MACHINE	
Model No.	Auto Graph AG 15
Range	0 - 50 *KN*
Accuracy	0.01 *N*
Location	Specimen preparation lab
Make	Shimadzu Japan
Applicable test	Tensile, Compressive, Flexural, Tear, Shear, Elongation & Modulus

3 Results and Discussion

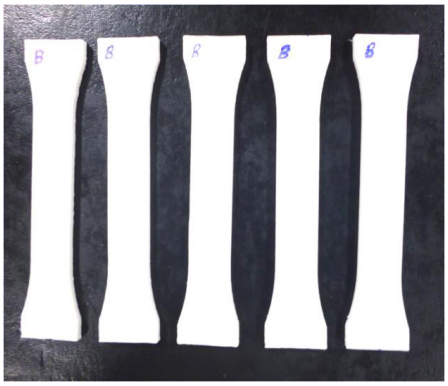

Fig. 13. 3D printed specimens for compressive testing

Fig. 13 shows the 3D printed ASTM D695 specimens tested on the UTM machine. The different loads applied for each specimen resulted in different graph points, with the highest

being 713.7 N and the lowest being 196.5 N, as shown in Fig. 14. Different graph points were obtained as each specimen behaved differently. There was also a variation in the load of 713.7 N, with breakage occurring before the yield point, which indicates the fragile nature of the material. Although all the specimens failed at different loads, the behavior of the specimens under compressive loading remained slightly related.

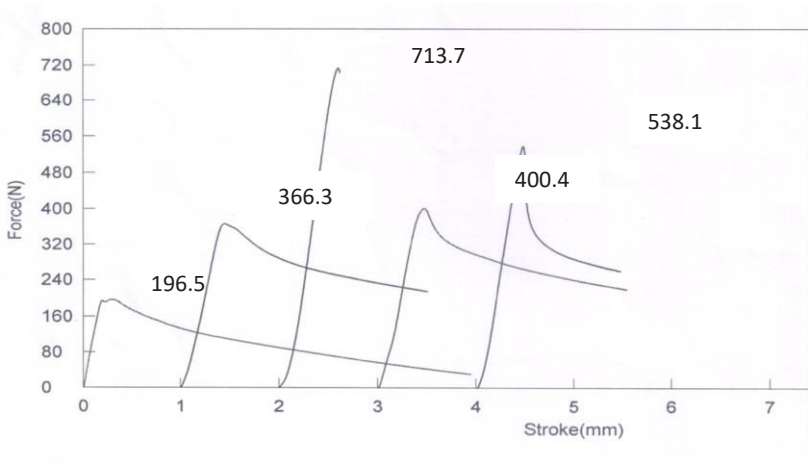

Fig. 14. Force vs stroke-compressive specimens

The results obtained from UTM experimental testing are presented in Table 7.

Table 7. Compressive Test Values

Specimen	Maximum force (N)	Maximum displacement (mm)	Maximum stress (N/mm^2)	Maximum strain (%)	Modulus (N/mm^2)
1-1	196.563	0.2890	4.16534	0.36430	2129.58
1-2	366.375	0..4455	7.69104	0.5620	1851.16
1-3	713.750	0.5990	15.0126	0.7549	2741.20
1-4	400.42	0.4790	8.4818	0.6033	2085.20
1-5	538.12	0.4860	11.3584	0.6127	2359.08
Mean	443.047	0.45970	9.32985	0.57848	2233.24

Variations were noticed in the results but were also in close proximity to the maximum and minimum displacements. The maximum and minimum stresses obtained were 15.0126 N/mm^2 and 4.1653 N/mm^2, respectively, and the maximum and minimum strains were 0.7549% and 0.3643%, respectively.

4 Conclusion

The fabrication of ASTM D695 specimens using PLA material was carried out on a Makerbot Replicator Z18 3D printer. The simulation and experimental validation of the compressive loading of 3D printed ASTM D695 PLA specimens were carried out using ANSYS software and a universal testing machine to find the compressive strength of the PLA material. The minimum equivalent stress of 1.617 N/mm^2 was detected at a 196.563 N load, and the maximum equivalent load of 19.144 N/mm^2 was detected at a 713.750 N load, and a maximum stress of 15.012 N/mm^2 was obtained at a 713.750 N load according to the UTM test results. A maximum deformation of 0.71 mm was noted for a load of 713.750 N

analytically, and a maximum deformation of 0.599 mm was obtained for a load of 713.750 N according to the UTM test results. Based on the analytical results, the minimum and maximum elastic strains were 0.09% at 196.563 N load and 1.06% at 713.750 N load respectively. Comparatively, a maximum elastic strain of 0.75 % was obtained at 713.750 N in the UTM tests. Based on the analysis, the behavior of specimen 3 was viewed as different due to the fragile nature of PLA, which caused early failure at a 713.7 N load. It was also observed that the obtained compressive strength of 15.01 N/mm^2 was close to the standard strength of 17.9 N/mm^2 [28], [29] which validates the results obtained from this study. Therefore, PLA parts printed using FDM can be used for various applications involving compressive loads.

References

1. P. Chennakesava and Y. S. Narayan, "Fused Deposition Modeling-Insights," *International Conference on Advances in Design and Manufacturing*, vol. 14, 2014.
2. A. Ramya and S. L. Vanapalli, "3D printing technologies in various applications," *Int J Mec Eng Technol*, vol. 7, no. 3, 2016.
3. D. Dimitrov, W. Van Wijck, K. Schreve, and N. De Beer, "Investigating the achievable accuracy of three-dimensional printing," *Rapid Prototyp J*, vol. 12, no. 1, 2006, doi: 10.1108/13552540610637264.
4. L. McLoughlin *et al.*, "Virtual sculpting and 3D printing for young people with disabilities," *IEEE Comput Graph Appl*, vol. 36, no. 1, 2016, doi: 10.1109/MCG.2016.1.
5. S. C. Joshi and A. A. Sheikh, "3D printing in aerospace and its long-term sustainability," *Virtual Phys Prototyp*, vol. 10, no. 4, 2015, doi: 10.1080/17452759.2015.1111519.
6. S. Shaffer, K. Yang, J. Vargas, M. A. Di Prima, and W. Voit, "On reducing anisotropy in 3D printed polymers via ionizing radiation," *Polymer*, vol. 55, no. 23, 2014, doi: 10.1016/j.polymer.2014.07.054.
7. O. S. Es-Said, J. Foyos, R. Noorani, M. Mendelson, R. Marloth, and B. A. Pregger, "Effect of layer orientation on mechanical properties of rapid prototyped samples," *Mater Manuf Process*, vol. 15, no. 1, 2000, doi: 10.1080/10426910008912976.
8. P. More, "3D Printing making the digital real," *Int J Eng Sci Res Technol*, vol. 2, no. 7, 2013.
9. C. Casavola, A. Cazzato, V. Moramarco, and C. Pappalettere, "Orthotropic mechanical properties of fused deposition modelling parts described by classical laminate theory," *Mater Des*, vol. 90, 2016, doi: 10.1016/j.matdes.2015.11.009.
10. O. A. Mohamed, S. H. Masood, and J. L. Bhowmik, "Optimization of fused deposition modeling process parameters: a review of current research and future prospects," *Adv Manuf*, vol. 3, no. 1, 2015, doi: 10.1007/s40436-014-0097-7.
11. B. M. Tymrak, M. Kreiger, and J. M. Pearce, "Mechanical properties of components fabricated with open-source 3-D printers under realistic environmental conditions," *Mater Des*, vol. 58, pp. 242–246, Jun. 2014, doi: 10.1016/j.matdes.2014.02.038.
12. M. Domingo-Espin, J. M. Puigoriol-Forcada, A. A. Garcia-Granada, J. Llumà, S. Borros, and G. Reyes, "Mechanical property characterization and simulation of fused deposition modeling Polycarbonate parts," *Mater Des*, vol. 83, 2015, doi: 10.1016/j.matdes.2015.06.074.
13. F. Ning, W. Cong, Y. Hu, and H. Wang, "Additive manufacturing of carbon fiber-reinforced plastic composites using fused deposition modeling: Effects of process parameters on tensile properties," *J Compos Mater*, vol. 51, no. 4, 2017, doi: 10.1177/0021998316646169.

14. A. Lanzotti, M. Grasso, G. Staiano, and M. Martorelli, "The impact of process parameters on mechanical properties of parts fabricated in PLA with an open-source 3-D printer," *Rapid Prototyp J*, vol. 21, no. 5, 2015, doi: 10.1108/RPJ-09-2014-0135.
15. E. Ulu, E. Korkmaz, K. Yay, O. Burak Ozdoganlar, and L. Burak Kara, "Enhancing the structural performance of additively manufactured objects through build orientation optimization," *J Mec Des*, vol. 137, no. 11, 2015, doi: 10.1115/1.4030998.
16. J. M. Chacón, M. A. Caminero, E. García-Plaza, and P. J. Núñez, "Additive manufacturing of PLA structures using fused deposition modelling: Effect of process parameters on mechanical properties and their optimal selection," *Mater Des*, vol. 124, 2017, doi: 10.1016/j.matdes.2017.03.065.
17. M. S. Hossain, J. Ramos, D. Espalin, M. Perez, and R. Wicker, "Improving tensile mechanical properties of FDM-manufactured specimens via modifying build parameters," in *24th International SFF Symposium - An Additive Manufacturing Conference, SFF 2013*, 2013.
18. S. Fehri, P. Cinelli, I. Anguillesi, and A. Lazzeri, "Thermal Properties of Plasticized Poly (Lactic Acid) (PLA) Containing Nucleating Agent," *Int J Chem Eng App*, vol. 7, no. 2, pp. 85–88, 2016.
19. J. Torres, M. Cole, A. Owji, Z. DeMastry, and A. P. Gordon, "An approach for mechanical property optimization of fused deposition modeling with polylactic acid via design of experiments," *Rapid Prototyp J*, vol. 22, no. 2, 2016, doi: 10.1108/RPJ-07-2014-0083.
20. T. Letcher and M. Waytashek, "Material property testing of 3D-printed specimen in pla on an entry-level 3D printer," in *ASME International Mechanical Engineering Congress and Exposition, Proceedings (IMECE)*, 2014. doi: 10.1115/IMECE2014-39379.
21. M. Jamshidian, E. A. Tehrany, M. Imran, M. Jacquot, and S. Desobry, "Poly-Lactic Acid: Production, applications, nanocomposites, and release studies," *Compr Rev Food Sci Food Saf*, vol. 9, no. 5, 2010, doi: 10.1111/j.1541-4337.2010.00126.x.
22. M. Bijarimi, S. Ahmad, and R. Rasid, "Mechanical, Thermal and Morphological Properties of PLA / PP Melt Blends," in *International Conference on Agriculture, Chemical and Environmental Sciences (ICACES'2012) Oct. 6-7, 2012 Dubai (UAE)*, 2012, pp. 115–117.
23. A. M. Clarinval and J. Halleux, "Classification of biodegradable polymers," in *Biodegradable Polymers for Industrial Applications*, 2005. doi: 10.1533/9781845690762.1.3.
24. M. Ashby and K. Johnson, *Materials and design: The art and science of material selection in product design*. 2014. doi: 10.1016/C2011-0-05518-7.
25. D. E. Henton, P. Gruber, J. Lunt, and J. Randall, "Polylactic acid technology," in *Natural Fibers, Biopolymers, and Biocomposites*, 2005. doi: 10.1002/1521-4095(200012)12:23<1841::aid-adma1841>3.3.co;2-5.
26. Subhani. A, "Influence of the process parameters on the properties of the polylactides based bio and eco-biomaterials," National Polytechnic Institute of Toulouse, 2011.
27. ASTM, "ASTM D695: Standard Test Method for Compressive Properties of Rigid Plastics," *ASTM International*, vol. 08, no. April 2003, 2002.
28. "Comparison of typical 3D printing materials,"
29. Makerbot, "PLA and ABS Strength Data ASTM D256, D695, D638, D790," *Makerbot*. New York.